

# Analysis of Urban Areas with Built-up Land Index Using ALOS PALSAR-2 Satellite Imagery (Case Study: Surabaya City)

*Muhammad Nabil Hadjoe<sup>1</sup>, Filsa Bioresita<sup>1\*</sup>, Noorlaila Hayati<sup>1</sup>, and Timo Balz<sup>2</sup>*

<sup>1</sup> Department Geomatics Engineering, Faculty of Civil, Planning, and Geo Engineering, Sepuluh Nopember Institute of Technology, Surabaya, Indonesia

<sup>2</sup> State Key Laboratory of Information Engineering in Surveying, Mapping and Remote Sensing, Wuhan University, Wuhan, China

\* Corresponding author: [filsa.bioresita@its.ac.id](mailto:filsa.bioresita@its.ac.id)

**Abstract.** Surabaya, the largest metropolitan city in East Java Province, has experienced rapid urban growth driven by population increase, economic development, and migration from surrounding regions. This growth has accelerated the expansion of built-up areas, particularly in suburban zones that were previously dominated by productive land such as rice fields and forests. These land use changes present significant challenges for sustainable urban spatial management, highlighting the need for efficient and reliable monitoring techniques. This study employs Synthetic Aperture Radar (SAR) based remote sensing, which enables consistent data acquisition regardless of weather conditions or illumination. ALOS PALSAR-2 Single Look Complex (SLC) data were utilized and analyzed using the SAR-based Impervious Built-up Index (IBUlsar) method to identify and map built-up areas based on backscatter characteristics. The application of the IBUlsar method aims to produce an accurate spatial distribution map of built-up land in Surabaya. The results indicate that higher IBUlsar values are concentrated in the city center and areas with intensive development activities. This information is expected to support urban spatial planning and contribute to sustainable urban development strategies.

# 1 Introduction

Surabaya as the largest metropolitan city in East Java Province has experienced significant growth, becoming a center of migration for people from surrounding areas [1]. Rapid economic growth and the availability of adequate infrastructure and facilities are the main factors behind the increase in population and the expansion of built-up areas [2]. This growth has led to notable land-use changes, especially in peri-urban areas that previously consisted of agricultural fields or forested land but have now been converted into residential areas and supporting urban facilities. Rising population density continues to pressure land resources, resulting in further land-use transformation to accommodate housing and public services [3]. The expansion of urban infrastructure has also intensified land demand and accelerated changes in urban land patterns.

In the context of monitoring built-up areas, remote sensing technology offers an efficient and effective approach. Among these, Synthetic Aperture Radar (SAR) stands out for its strong capability to observe highly developed urban environments. SAR can overcome common limitations of optical imagery, such as cloud cover, atmospheric disturbances, and dependence on sunlight [4]. Its ability to operate regardless of weather conditions further enhances its utility for continuous monitoring. Moreover, SAR's geometric sensitivity allows for more accurate extraction of surface characteristics [5].

Urban area identification using SAR data can be performed through SAR-based built-up indices. One method that has shown strong potential is the Impervious Built-up Index (IBUIsar) introduced by [6]. This index relies on radar backscatter information to improve the detection of urban surfaces. The study by [6] showed that IBUIsar, which utilizes ALOS PALSAR imagery, was able to extract built-up areas in three locations with overall accuracies of 90%, 98%, and 87.6% respectively. This highlights the effectiveness of the method as a reliable approach for mapping built-up surfaces.

Detecting urban built-up areas through built-up index algorithms represents a key method in mapping urbanization patterns. Previous studies have shown that the use of SAR for detecting built-up areas still faces challenges such as speckle, backscatter variations, and limited spectral information [7], [8], [9]. Several studies have combined SAR and optical data [10], [11], [12], [13], but the results remain dependent on the quality of the optical imagery. Meanwhile, built-up index approaches such as NDBI, EBI, and UI [14], [15] are mostly effective only for optical imagery and are less optimal when applied to SAR data.

This study employs ALOS PALSAR-2 imagery using the IBUIsar built-up index, which combines dual-polarization data (HH and HV) to enhance the differentiation of urban surfaces. IBUIsar utilizes radar backscatter information to more accurately identify built-up features. This research aims to analyze urban areas using a built-up index to obtain clearer and more reliable information on urban characteristics.

## 2 Methods

### 2.1 Study Area

The research is located in Surabaya City, East Java Province, as shown in Figure 1. Geographically, The city of Surabaya borders Gresik Regency to the west and the Madura Strait to the north and east.

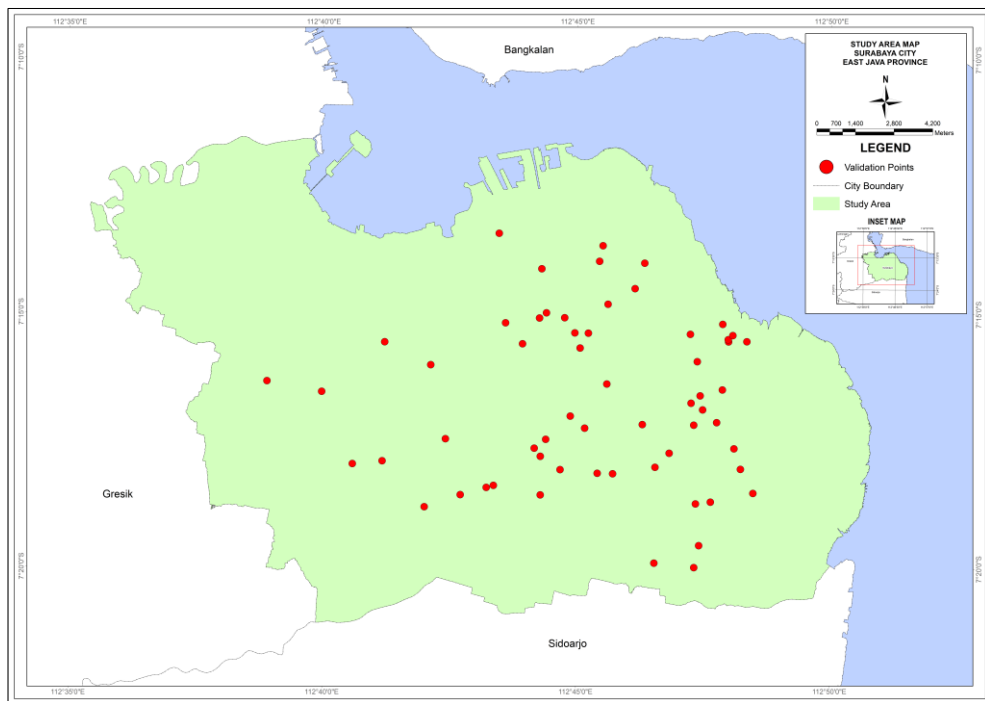


**Fig. 1.** Study Area

### 2.2 Dataset

In this study, the instruments used include satellite imagery, vector spatial data, and field observation data. The primary instrument is ALOS PALSAR-2 SLC dual-polarization (HH + HV) imagery, which provides a spatial resolution of approximately 10 m and a temporal resolution (revisit time) of about 14 days, allowing consistent observation of surface characteristics and changes over time. This data is consisting of 2 scenes acquired in 2022

and 2024. In addition to satellite data, a shapefile of the administrative boundary of Surabaya City was utilized. To validate the results of the image processing, field observations (ground truth) and Google Earth data were employed as reference sources for comparison with the built-up land index classification outcomes.

### 2.3 Method

The processing stage began with the use of ALOS PALSAR-2 imagery to calculate the radar-based Built-up Index (IBUIsar), which utilizes backscatter values from HH and HV polarizations to identify built-up areas. The first step involved preprocessing the ALOS PALSAR-2 data using SNAP software. The raw Single Look Complex (SLC) SAR data were converted into power or intensity data. A multi-looking operation was then applied to reduce speckle noise and enhance the signal-to-noise ratio, while slightly decreasing spatial resolution. The azimuth-to-range look ratio was set at 3:1 to optimize speckle reduction, as this ratio represents a practical compromise between reducing speckle noise and preserving spatial resolution, thereby improving radiometric stability without excessively degrading the geometric quality of urban features [14]. Radiometric calibration was subsequently performed to convert digital number values into backscatter coefficients ( $\sigma^0$ ), ensuring that the data have consistent physical meaning across time and space. To further refine the image, a Gamma Map filter with a 3×3 moving window was applied for additional speckle suppression without compromising critical spatial details. Geocoding and terrain correction were then conducted using a Digital Elevation Model (DEM) to correct geometric distortions caused by terrain variations and to accurately project the imagery into the UTM-WGS84 coordinate system. The process employed the Range-Doppler terrain correction approach with SRTM DEM resampled to a 25 m pixel size using the nearest neighbor method. The final calibrated and corrected backscatter data were clipped to the administrative boundary of Surabaya City to prepare the dataset for subsequent classification and analysis.

The next step is to calculate the built-up land index (IBUIsar). The index value is calculated based on a mathematical combination of HH and HV backscatter values that describe the intensity of the impervious surface. The calculation involves three main components: first, parameter **a** represents the normalized difference between HH and HV backscatter (Eq. 2), emphasizing the relative contrast of surface scattering; second, parameter **b** expresses the direct ratio of HH to HV backscatter (Eq. 3), which reflects the surface roughness and orientation characteristics. These two parameters are then combined in an exponential normalization form, producing the final IBUIsar equation [14]:

$$IBUIsar = a - \frac{(e^a - e^b)}{(e^a + e^b)} \quad (1)$$

$$a = \frac{(HH_{\sigma}^0 - HV_{\sigma}^0)}{(HH_{\sigma}^0 + HV_{\sigma}^0)} \quad (2)$$

$$b = \left[ \frac{(HH^0_\sigma)}{(HV^0_\sigma)} \right] \quad (3)$$

This formulation enhances the distinction between built-up and non built-up features. Negative or near-zero IBUsar values typically indicate built-up areas, while positive values correspond to vegetation, bare soil, or water surfaces.

The accuracy of the built-up area classification was assessed using a confusion matrix to compare both indices against the validation data, employing 30 validation points representing built-up areas and 30 validation points representing non built-up areas. The selected points represent areas that remained unchanged in 2022 and 2024.

### 3 Result and Discussion

#### 3.1 Result

The preprocessing stage of the ALOS PALSAR-2 imagery produced calibrated backscatter values ( $\sigma^0$ ) for both HH and HV polarizations, which serve as the fundamental inputs for generating the IBUsar index. These backscatter signals reflect the interaction between radar energy and surface features, allowing differentiation between built-up areas and other land-cover types based on their scattering characteristics.

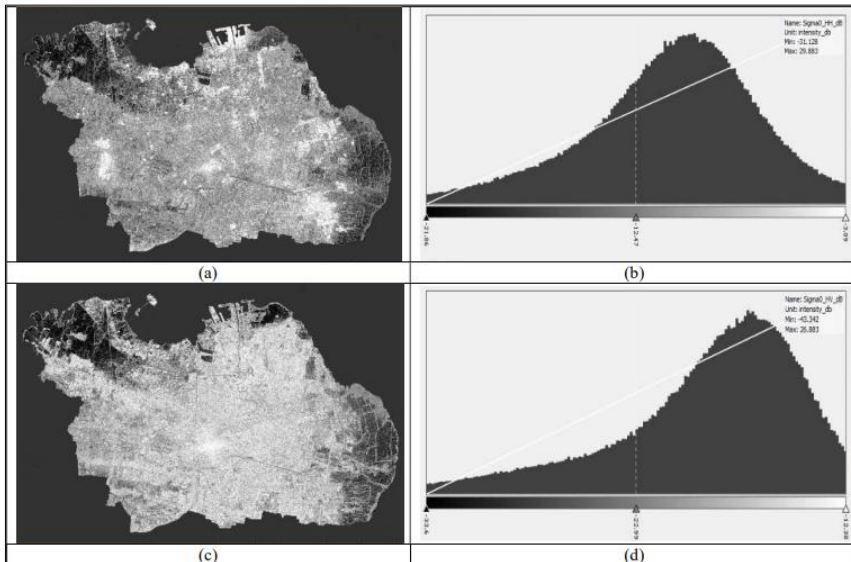


**Fig. 2.** ALOS PALSAR-2 backscatter in 2022, (a) HH polarization, (b) histogram of HH polarization, (c) HV polarization, (d) histogram of HV polarization

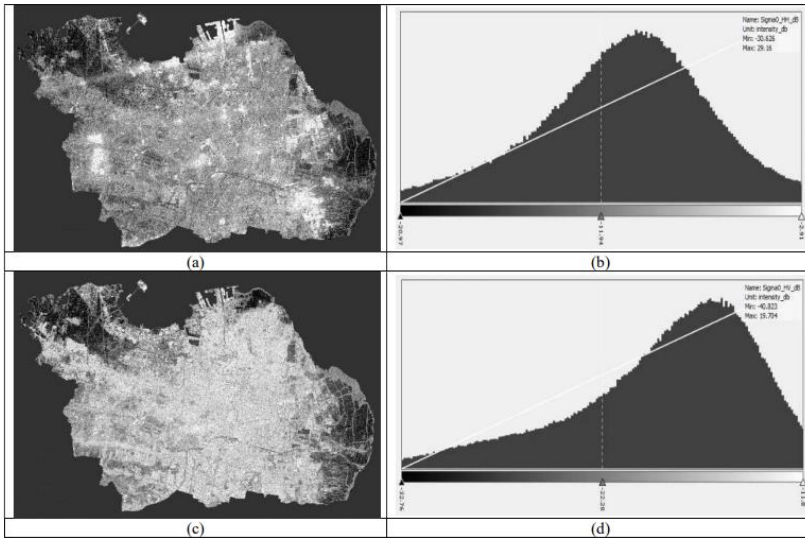


**Fig. 3.** ALOS PALSAR-2 backscatter in 2024, (a) HH polarization, (b) histogram of HH polarization, (c) HV polarization, (d) histogram of HV polarization

The backscatter  $\sigma^0$  ALOS PALSAR-2 value range in 2022 (Figure 2) and 2024 (Figure 3) shows a clear difference in dispersion response between HH and HV polarizations, which can be directly related to surface and land-cover characteristics. In 2022, HH values ranged from  $-31.128$  to  $29.883$  dB (Figure 2b), where high HH values are typically associated with strong surface and double-bounce scattering from built-up areas and other hard surfaces, while low values correspond to smooth surfaces such as water bodies or bare land. In contrast, HV values ranged from  $-43.342$  to  $26.883$  dB (Figure 2d), indicating a mixture of very low returns from smooth surfaces and very high returns from hard objects or urban structures. In 2024, HH values showed a similar range, from  $-30.626$  to  $29.16$  dB (Figure 3b), indicating the continued presence of stable hard surfaces and urban features. Meanwhile, HV values range decreased from  $-40.823$  to  $19.704$  dB (Figure 3d), suggesting a reduced contribution of volume scattering, potentially due to changes in vegetation cover or increased dominance of surface scattering. The consistent maximum HH values across both years highlight the persistence of built-up areas, whereas the reduced HV response in 2024 indicates changes in land cover that affect vegetation-related and complex structural scattering mechanisms.

The IBUlsar algorithm is formulated using normalized combinations of HH and HV backscatter values to improve the separation between built-up and non built-up. By calculating the mean and standard deviation (SD) of the IBUlsar output across different land-cover types, the index demonstrates a strong ability to isolate built-up areas from other classes. Built-up pixels consistently show negative or near-zero IBUlsar values, while non built-up areas such as vegetation, bare soil, and water surfaces produce positive values

without overlap in the SD range. This clear separation allows the classification threshold to be determined directly from the distribution of IBUIsar values. Following the approach in a previous study [14], the threshold is adopted by assigning negative IBUIsar values to built-up areas and positive values to non built-up areas. The IBUIsar algorithm result in 2022 and 2024 is shown in Figure 4.

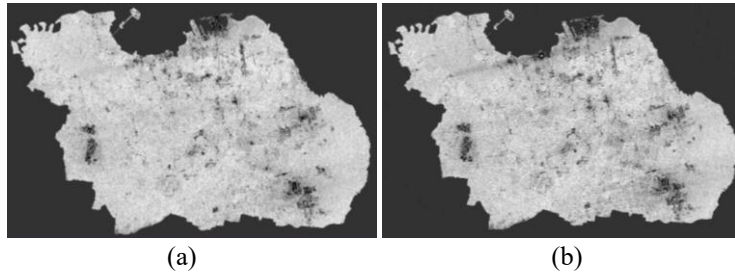


**Fig. 4.** IBUIsar Algorithm Results in 2022 (a) and 2024 (b)

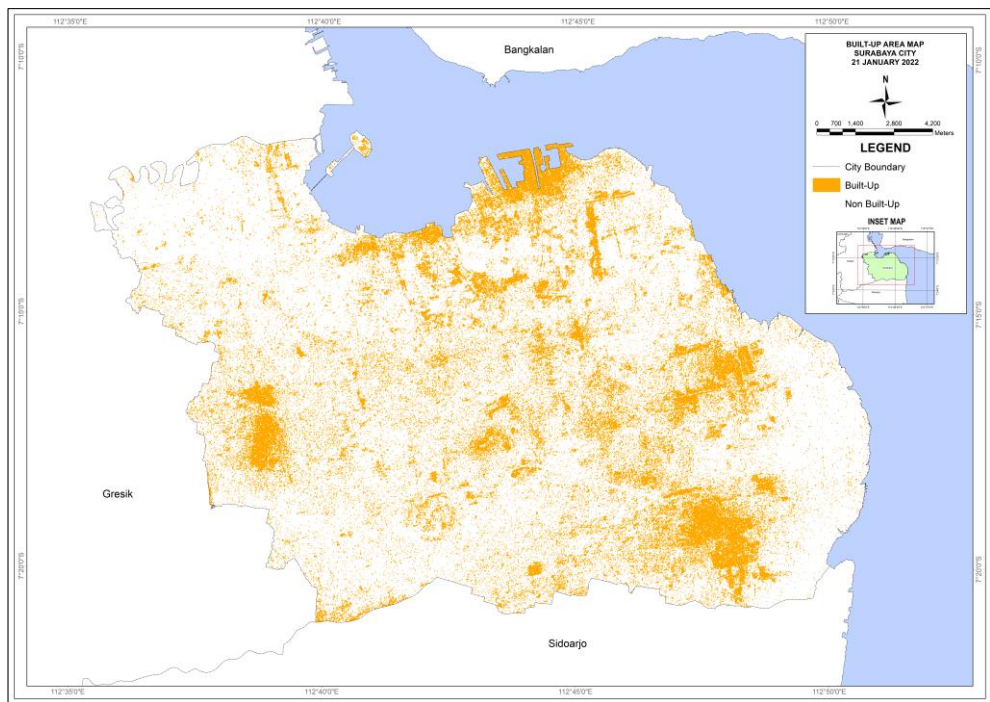


**Fig. 5.** Built-up Area Map of Surabaya City in 2022

Figure 5 presents the built-up area map of Surabaya City in 2022, shows two classification categories represented by distinct colours. The map is predominantly shaded in no colour, indicating that non built-up areas occupy most of the city's surface. Built-up areas, shown in orange pixel are concentrated in central, eastern, and northern parts of Surabaya, with denser patterns visible around industrial zones and the port area along the northern coastline. Smaller clusters of built-up pixels also appear in the western and southern sections, reflecting mixed land-use characteristics.

Similar to previous years, figure 6 shows a map of built-up areas in Surabaya in 2024. This map is dominated by no colour, indicating that non built-up areas still dominate most of Surabaya's land area. Built-up areas, shown in orange pixel, form dense concentrations in the center, east, and north of the city, with significant intensification around industrial areas and port complexes along the north coast. Additional clusters of built-up areas are also visible in the west and south, reflecting ongoing urban expansion and diverse land use patterns in the city's suburbs.

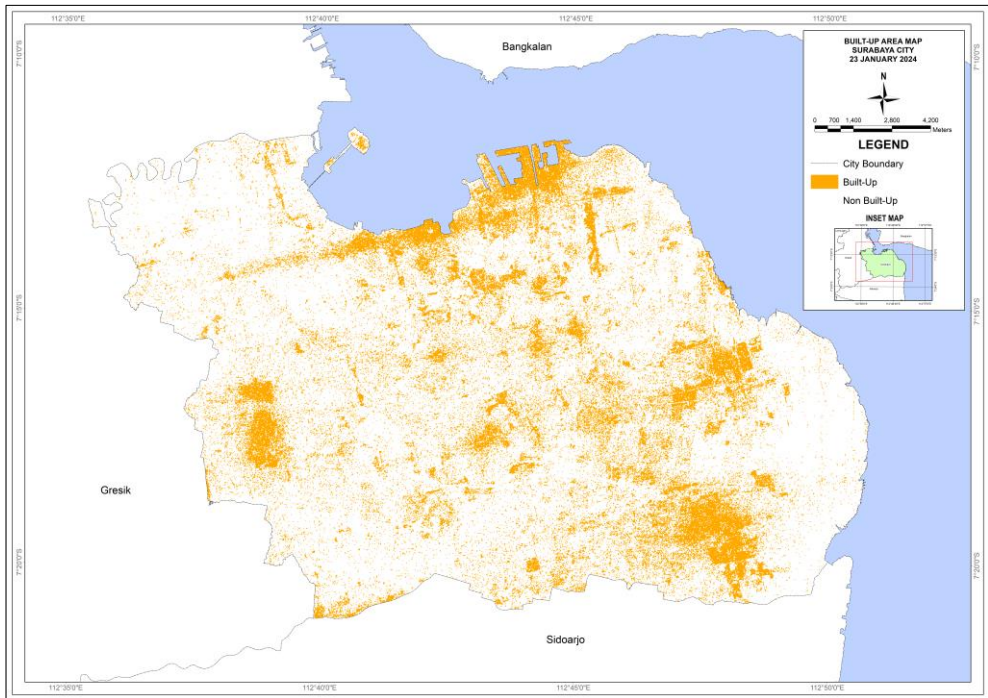


**Fig. 6.** Built-up Area Map of Surabaya City in 2024

A comparison of the areas in 2022 and 2024 indicates a slight change in the distribution of built-up and non-built-up areas in the city of Surabaya. In 2022, the built-up area was

recorded at around 6,429.360 ha, slightly higher than in 2024, which reached 5,899.696 ha. This decrease may indicate a change in classification for several pixels that were previously detected as built-up but were later identified as non-built-up, mainly due to backscatter variations or differences in surface conditions. Meanwhile, the area of non-built-up land increased from 27,157.394 ha in 2022 to 27,684.249 ha in 2024. Overall, these changes reflect relatively stable urban surface dynamics with insignificant shifts in area over a two-year period.

The accuracy assessment was carried out using 60 validation points, consisting of 30 points representing built-up areas and 30 points representing non-built-up areas. All validation points were selected from locations that remained unchanged between 2022 and 2024 to ensure consistency in evaluating the index performance. Based on the confusion matrix shown in Table 1, the IBUIsar algorithm demonstrates a strong ability to separate built-up from non built-up areas. In 2022, the method achieved an overall accuracy of 86.67%, while in 2024 the accuracy increased to 90%, indicating improved classification reliability. The index also shows consistently better performance in detecting built-up areas, suggesting that the backscatter-based formulation effectively captures the scattering characteristics of impervious surfaces. Meanwhile, misclassifications in non-built-up areas are likely influenced by surface heterogeneity and local backscatter variations, highlighting the importance of stable validation points in ensuring reliable accuracy estimation.

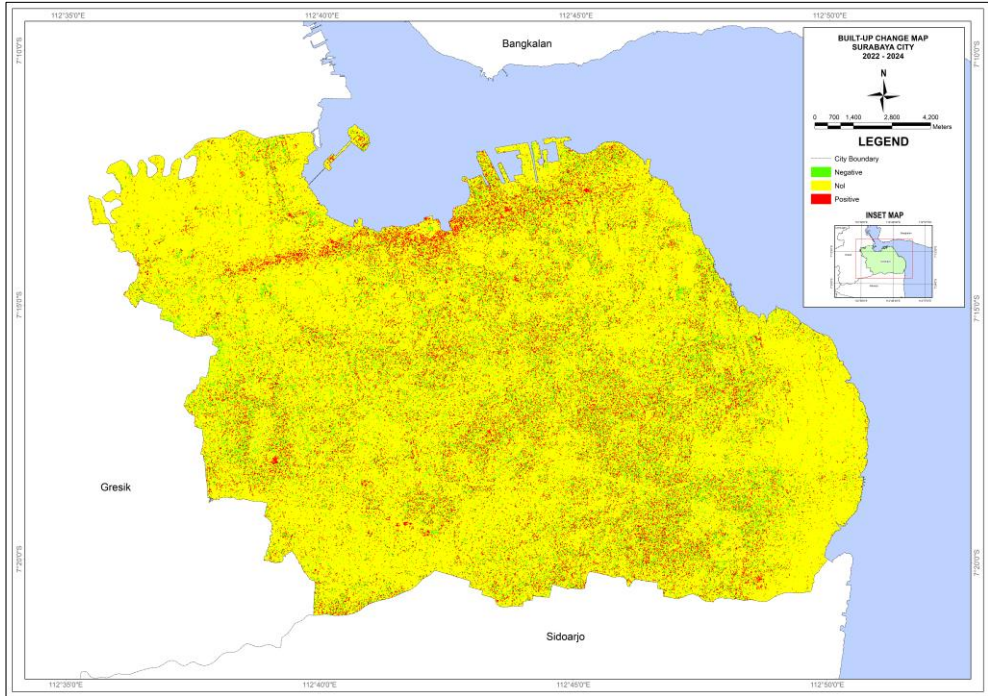
**Table 1.** Confusion Matrix Result

Year	Predict	Actual		Total	Accuracy (%)
		Built-up	Non Built-up		
2022	Built-up	25	3	28	86.67%
	Non Built-up	5	27	32	
	Total	30	30	60	
2024	Built-up	24	0	24	90.00%
	Non Built-up	6	30	36	
	Total	30	30	60	

### 3.2 Discussion

The identification of built-up areas in Surabaya using ALOS PALSAR-2 imagery from 2022 and 2024 provides an overview of the city's development dynamics over two years. IBUIsar based analysis was used to distinguish between built-up and non-built-up areas, while also evaluating the consistency of the algorithm in complex urban environments. The comparison between the two years not only shows patterns of change in the city's surface,

but also helps assess the extent to which IBUlsar is able to represent actual conditions in the field.



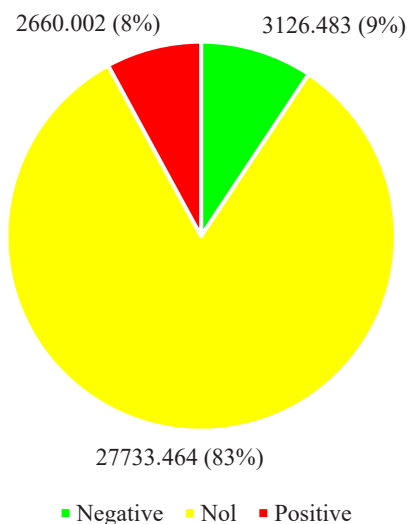
**Fig. 7.** Built-up Area Change Map 2022 and 2024 of Surabaya City

Figure 7 illustrates the built-up area change in Surabaya City between 2022 and 2024, derived from the IBUlsar built-up land index. The map categorizes change into three classes: positive change, negative change, and no change. Areas marked in red represent positive change, indicating locations that were classified as non built-up in 2022 but transitioned into built-up by 2024. The positive change extending across the northern part of Surabaya from east to west is likely influenced by a combination of physical surface conditions and limitations of the IBUlsar method. This area is dominated by port activities, industrial zones, and coastal infrastructure characterized by hard surfaces that generate high backscatter and are therefore prone to being detected as built-up areas. However, the clear linear pattern also suggests the influence of backscatter variations related to surface moisture, tidal conditions, or radar acquisition geometry, indicating that part of the detected positive change may reflect

the sensitivity of IBUlsar to coastal and industrial environments rather than actual new urban expansion.

Areas shown in green correspond to negative change, where land previously identified as built-up in 2022 shifted to non built-up in 2024. These pixels are relatively dispersed and appear in small patches, reflecting inconsistencies likely arising from the IBUlsar classification rather than actual land-cover reduction.

Meanwhile, the yellow pixels dominate the map, representing no change between the two years. However, the overwhelming extent of this yellow class, especially in areas that are known to be highly urbanized, indicates potential misclassification in the 2024 IBUlsar output. Overall, the spatial pattern suggests that the algorithm did not fully capture the true extent of built-up development in Surabaya, as evidenced by unexpectedly large zones labeled as unchanged non built-up.



**Fig. 8.** Area Proportions of Built-up Change in Surabaya (2022 and 2024)

According to Figure 8, the results of the area proportion show that most of Surabaya, around 83%, did not experience any changes between 2022 and 2024 according to the IBUlsar algorithm. Areas that experienced negative changes, namely those that shifted from built-up to non built-up, covered around 9% of the total area. Meanwhile, areas with positive changes, namely changes from non built-up in 2022 to built-up in 2024, only cover about 8%. This distribution indicates that the majority of the area remains in the same condition,

while the detected changes are relatively small and likely reflect the limitations of the accuracy of the IBUIsar classification in 2024.

The overall findings of this study highlight both the potential and the limitations of using the IBUIsar index derived from ALOS PALSAR-2 data for identifying built-up areas in Surabaya. While the method provides a general indication of surface conditions and captures certain patterns of urban expansion, inconsistencies particularly in the 2024 classification show that the algorithm still requires refinement to better reflect real world urban characteristics. The minimal proportion of detected changes and the unexpected dominance of non built-up classifications in heavily urbanized zones suggest that the index alone is insufficient for detailed urban monitoring. Future research would benefit from integrating additional SAR or optical datasets, adjusting thresholding methods, and incorporating more robust validation points to enhance the reliability and accuracy of built-up area detection in complex urban environments.

## **4 Conclusion**

The IBUIsar index derived from ALOS PALSAR-2 imagery is able to provide a general overview of the distribution of built-up areas in Surabaya in 2022 and 2024, but its accuracy remains limited for more detailed urban analysis. The decrease in built-up area from approximately 6,429.360 ha in 2022 to 5,899.696 ha in 2024, the dominance of unchanged areas, and the appearance of unexpected classifications in several urban zones indicate inconsistencies in the algorithm, which are more related to weaknesses in threshold determination and the sensitivity of IBUIsar to dense urban areas rather than actual surface-cover changes. Therefore, this method requires improvements through threshold calibration, incorporation of supporting datasets, and refinement of validation samples to produce more accurate and representative built-up area mapping.

## **Acknowledgment**

The authors would like to thank Japan Aerospace Exploration Agency (JAXA) via the 3rd Research Announcement on Earth Observation (ER3A2N511) for providing ALOS PALSAR-2 imagery data in this study. This research is funded by the Indonesian Endowment Fund for Education (LPDP) on behalf of the Indonesian Ministry of Higher Education, Science and Technology and managed under the EQUITY Program (Contract No. 4299/B3/DT.03.08/2025 & No 3029/PKS/ITS/2025).

## References

- [1] F. Ramdhani, “Impact of Urbanization for City Developments in Indonesia,” 2013.
- [2] D. Fitria Pida, K. N. Aini, and C. A. Putri, “Dampak Urbanisasi terhadap Perkembangan Kota di Indonesia: Tinjauan dari Aspek Ekonomi Pembangunan,” vol. 3, no. 1, pp. 226–238, 2025, doi: 10.62383/wissen.v3i1.562.
- [3] K. H. Rahmani and B. M. Sukojo, “Evaluation of the Suitability of Land Use and Building Based on BIM to Support the Spatial Planning of North Gandaria Village,” vol. 19, no. 1, pp. 96–105, 2023.
- [4] F. Fadlin, M. A. Thaha, F. Maricar, and M. P. Hatta, “Monitoring Perubahan Penggunaan Lahan Menggunakan Citra Satelit Sentinel 1 di DAS Wanggu Kota Kendari,” *Jurnal Teknik Sumber Daya Air*, vol. 1, no. 2, pp. 77–88, Jul. 2022, doi: 10.56860/jtsda.v1i2.5.
- [5] Y. Zhang, J. Zhang, H. Wu, Z. Lu, and S. Guangtong, “Monitoring of urban subsidence with SAR interferometric point target analysis: A case study in Suzhou, China,” *International Journal of Applied Earth Observation and Geoinformation*, vol. 13, no. 5, pp. 812–818, 2011, doi: 10.1016/j.jag.2011.05.003.
- [6] S. Sinha, A. Santra, and S. S. Mitra, “Semi-automated impervious feature extraction using built-up indices developed from space-borne optical and SAR remotely sensed sensors,” *Advances in Space Research*, vol. 66, no. 6, pp. 1372–1385, Sep. 2020, doi: 10.1016/j.asr.2020.05.040.
- [7] A. Maqsoom, B. Aslam, A. Yousafzai, F. Ullah, S. Ullah, and M. Imran, “Extracting built-up areas from spectro-textural information using machine learning,” *Soft comput*, vol. 26, no. 16, pp. 7789–7808, Aug. 2022, doi: 10.1007/s00500-022-06794-6.
- [8] T. Li *et al.*, “Built-Up Area Extraction from GF-3 SAR Data Based on a Dual-Attention Transformer Model,” *Remote Sens (Basel)*, vol. 14, no. 17, Sep. 2022, doi: 10.3390/rs14174182.
- [9] H. B. Makineci, “Spatio-temporal change detection of built-up areas with Sentinel-1 SAR data using random forest classification for Arnavutköy Istanbul,” *Niğde Ömer Halisdemir Üniversitesi Mühendislik Bilimleri Dergisi*, vol. 12, no. 2, pp. 626–636, 2023, doi: 10.28948/ngmuh.1203301.
- [10] B. Shrestha, H. Stephen, and S. Ahmad, “Impervious surfaces mapping at city scale by fusion of radar and optical data through a random forest classifier,” *Remote Sens (Basel)*, vol. 13, no. 15, Aug. 2021, doi: 10.3390/rs13153040.
- [11] Y. Forget, M. Shimoni, M. Gilbert, and C. Linard, “Complementarity Between Sentinel-1 and Landsat 8 Imagery for Built-Up Mapping in Sub-Saharan Africa,” *Polymer Preprints*, no. 2018100695, Oct. 2018, doi: 10.20944/preprints201810.0695.v1.
- [12] R. Azmi, J. Chenal, H. Amar, C. S. Tekouabou Koumetio, and E. B. Diop, “A Hybrid Approach for Extracting Large-Scale and Accurate Built-Up Areas Using SAR and

- Multispectral Data,” *Atmosphere (Basel)*, vol. 14, no. 2, Feb. 2023, doi: 10.3390/atmos14020240.
- [13] W. Wu, S. Guo, Z. Shao, and D. Li, “CroFuseNet: A Semantic Segmentation Network for Urban Impervious Surface Extraction Based on Cross Fusion of Optical and SAR Images,” *IEEE J Sel Top Appl Earth Obs Remote Sens*, vol. 16, pp. 2573–2588, 2023, doi: 10.1109/JSTARS.2023.3250461.
- [14] T. A. Kebede, B. T. Hailu, and K. V. Suryabhagavan, “Evaluation of spectral built-up indices for impervious surface extraction using Sentinel-2A MSI imageries: A case of Addis Ababa city, Ethiopia,” *Environmental Challenges*, vol. 8, Aug. 2022, doi: 10.1016/j.envc.2022.100568.
- [15] F. Samadzadegan, A. Toosi, and F. Dadrass Javan, “Automatic built-up area extraction by feature-level fusion of LuoJia 1–01 nighttime light and Sentinel satellite imageries in Google Earth Engine,” *Advances in Space Research*, vol. 72, no. 4, pp. 1052–1069, Aug. 2023, doi: 10.1016/j.asr.2023.05.015.